

Supporting Information

Engineering the Surface of Carbon Dots for Enhanced Photoluminescence and Controlled Plasmonic Interactions

M. Reale¹, Z. Moussadjy¹, G. Buscarino^{1,2}, U. De Giovannini¹, A. Emanuele¹, M. Cannas¹, R. Cillari³, N. Mauro³, A. Sciortino^{1,2*}, F. Messina^{1,2*}

¹*Dipartimento di Fisica e Chimica “Emilio Segrè”, Università degli Studi di Palermo, Via Archirafi 36, Palermo 90123, Italy.*

²*ATeN Center, Università degli Studi di Palermo, Palermo, Italy.*

³*Dipartimento di Scienze e Tecnologie Biologiche, Chimiche e Farmaceutiche, Università degli Studi di Palermo, via Archirafi 32, Palermo 90123, Italy*

**Corresponding author E-mail: fabrizio.messina@unipa.it, alice.sciortino02@unipa.it*

Field Enhancement with Mie Theory

In this section, we detail the calculation of the near-field enhancement around a metallic sphere using Mie theory, focusing on the specific case where the incident plane wave propagates along the \hat{z} direction and is polarized along the \hat{x} axis. The formulation follows the approach presented in [1].

For simplicity, we restrict to the geometry of the problem in the plane of incidence ($\varphi = 0$) and therefore the spherical coordinates (r, θ, φ) are reduced to (r, θ) . The incident electric field in the plane of incidence can be expressed as:

$$\mathbf{E}_{inc} = E_0 e^{ikr\hat{x}} = E_0 e^{ikr\cos\theta} (\sin\theta \hat{e}_r + \cos\theta \hat{e}_\theta)$$

where k is the wave number and $\mathbf{k} = k\hat{z}$.

The incident field can be expanded in terms of vector spherical harmonics as:

$$\mathbf{E}_{inc} = \sum_{n=1}^{\infty} E_n [\mathbf{M}_n - i\mathbf{N}_n]$$

with coefficients:

$$E_n = E_0 i^n \frac{2n+1}{n(n+1)}$$

The vector spherical harmonics in the plane of incidence simplify to:

$$\mathbf{M}_n = \pi_n(\cos\theta) h_n^{(1)}(\rho) \hat{e}_\theta$$

$$\mathbf{N}_n = n(n+1) \sin\theta \pi_n(\cos\theta) \frac{h_n^{(1)}(\rho)}{\rho} \hat{e}_r + \tau_n(\cos\theta) \left[\frac{\rho h_n^{(1)}(\rho)}{\rho} \right]' \hat{e}_\theta$$

where $h_n^{(1)}(\rho)$ are spherical Hankel functions of the first kind with $\rho = kr$ and prime denote derivative with respect to the argument.

The angular functions π_n and τ_n are defined recursively:

$$\pi_n = \frac{2n-1}{n-1} \mu \pi_{n-1} - \frac{n}{n-1} \pi_{n-2}$$

$$\tau_n = n\mu\pi_n - (n+1)\pi_{n-1}$$

with initial conditions $\pi_0 = 0$ and $\pi_1 = 1$ and $\mu = \cos\theta$.

According to Mie theory the scattered field is given by:

$$\mathbf{E}_{sca} = \sum_{n=1}^{\infty} E_n [ia_n \mathbf{N}_n - b_n \mathbf{M}_n]$$

Where a_n and b_n are the Mie coefficients defined as:

$$a_n = \frac{m\psi_n(mx)\psi_n'(x) - \psi_n(x)\psi_n'(mx)}{m\psi_n(mx)\xi_n'(x) - \xi_n(x)\psi_n'(mx)}$$

$$b_n = \frac{\psi_n(mx)\psi_n'(x) - m\psi_n(x)\psi_n'(mx)}{\psi_n(mx)\xi_n'(x) - m\xi_n(x)\psi_n'(mx)}$$

where: $x = ka$ is the size parameter, with a being the radius of the sphere; $m = n_2/n_1$ is the relative refractive index of the sphere to the surrounding medium; $\psi_n(\rho) = \rho j_n(\rho)$ are Riccati-Bessel functions; $\xi_n(\rho) = \rho h_n^{(1)}(\rho)$ are Riccati-Hankel functions.

We define the near-field enhancement factor f as the ratio of the magnitude of the scattered electric field to the incident field amplitude:

$$f = \frac{|E_{sca}|}{E_o}$$

By calculating f at various points around the sphere, we obtain the spatial distribution of the near-field enhancement.

Supplementary Figures:

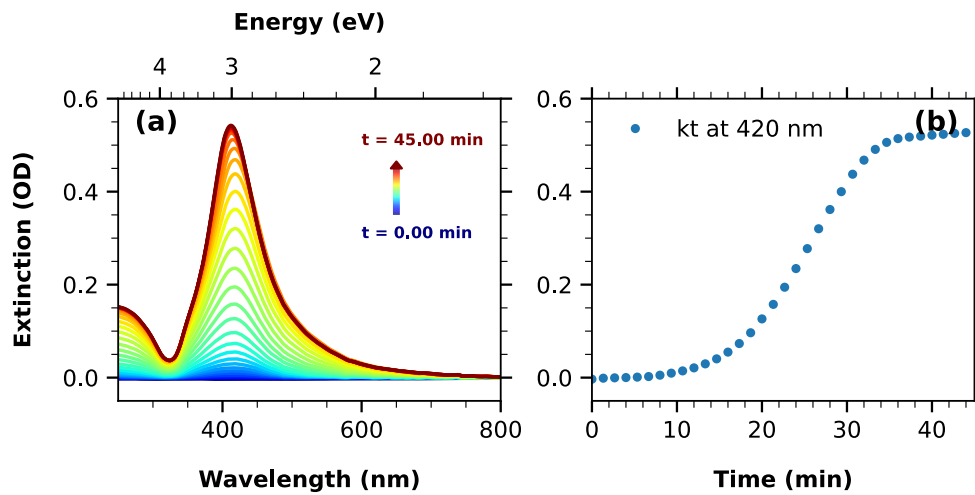


Figure S1: Real-time monitoring of AgNPs formation by the collection of (a) the UV-Vis spectra of the solution taken during the synthesis at equidistant time intervals from 0 to 45 min after starting the reaction. (b) Reaction kinetic obtained by plotting the signal at 420 nm extracted from data in (a) vs time.

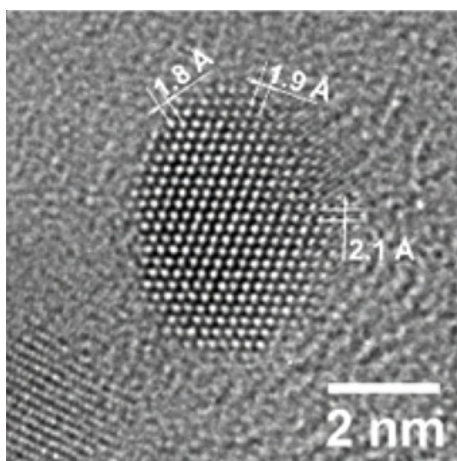


Figure S2: HR-TEM image of an individual CD, with the reported lattice parameters. Adapted from [2].

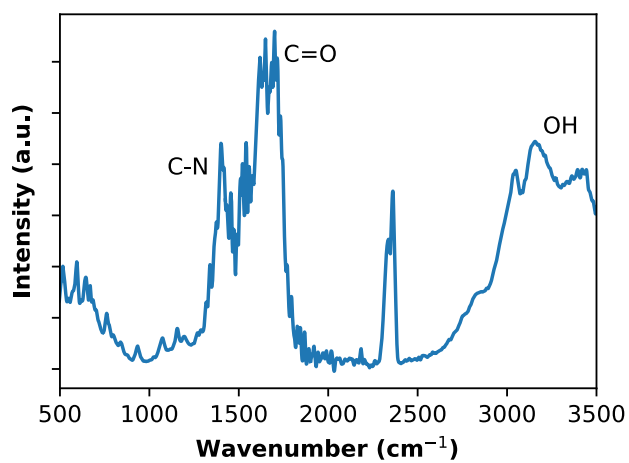


Figure S3: ATR infrared spectrum of CDs. Attribution of the main observed peaks to surface chemical groups on CDs are indicated by labels.

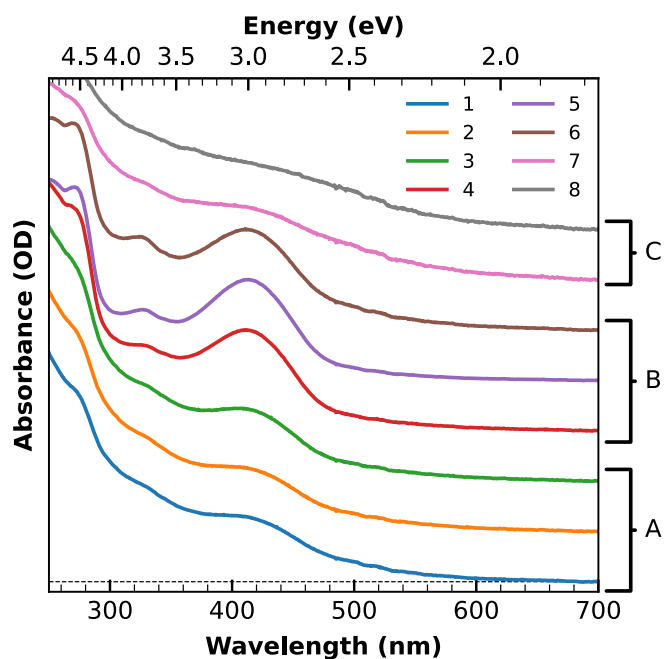


Figure S4: Absorption spectra of the different fractions extracted by chromatographic selection from solution of CDs after PEGylation reaction. Based on their spectral characteristics can be grouped into three main subset A, B and C. Fraction A corresponds to the PEGylated CDs.

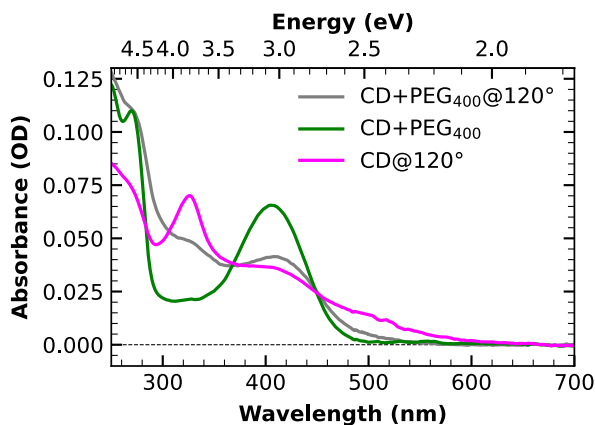


Figure S5: Comparison between the absorption spectrum of CDs after PEGylation reaction (grey), and of the reference samples obtained by simple PEG addition to CDs solution (green) and by thermal treatment of CDs without PEG addition (magenta).

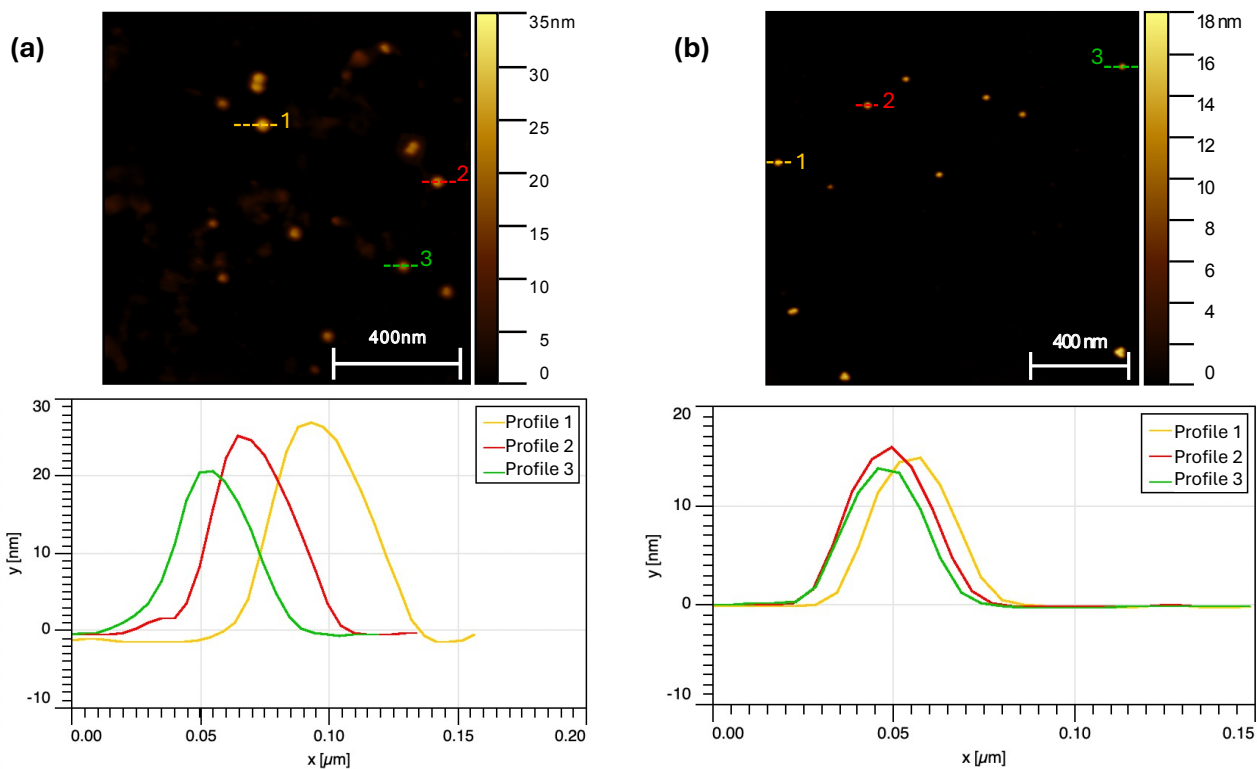


Figure S6: Horizontal z-profiles of representative (a) AgNPs and (b) AuNP, as obtained by AFM images.

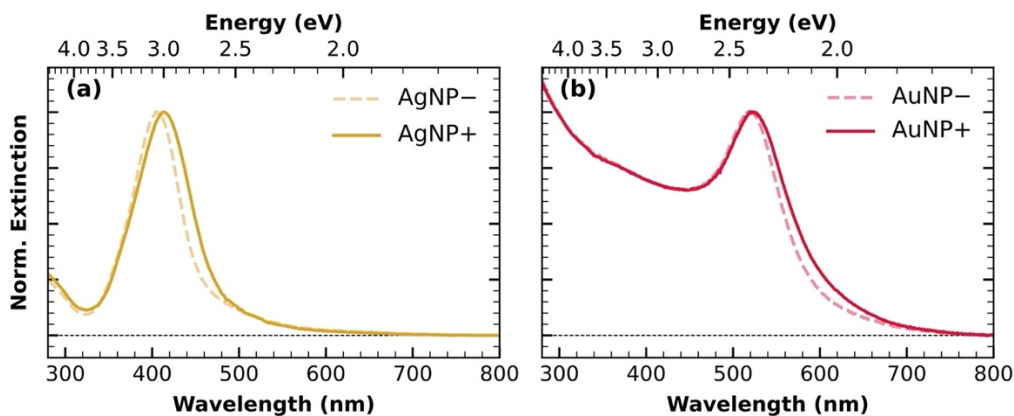


Figure S7: Extinction spectra of the starting gold nanoparticles ($AuNP^-$, in dashed yellow) and after the ligand-exchange procedure ($AuNP^+$, in continuous yellow). (b) Extinction spectra of the starting silver nanoparticle ($AgNP^-$, in dashed pink) and after the ligand-exchange procedure ($AuNP^+$, in continuous red).

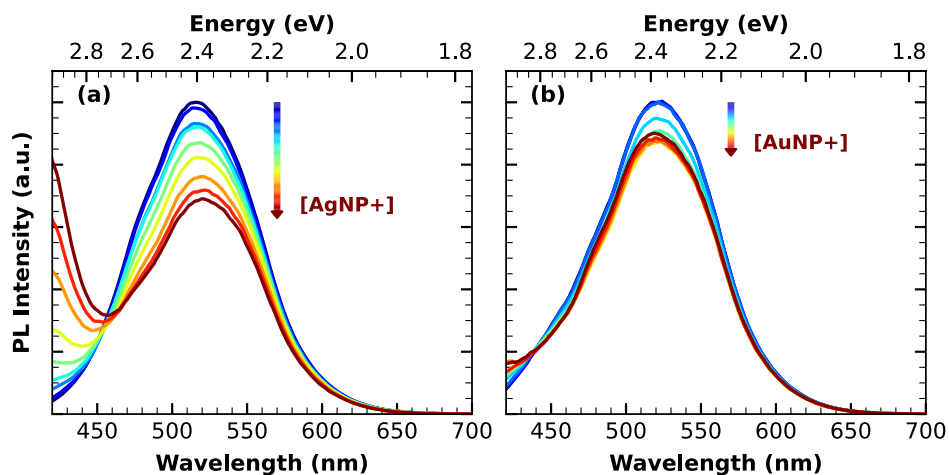


Figure S8: PL spectra of pristine CD aqueous solution under $\lambda_{exc} = 410 \text{ nm}$ upon increasing concentrations of (a) AgNP+ and (b) AuNP+.

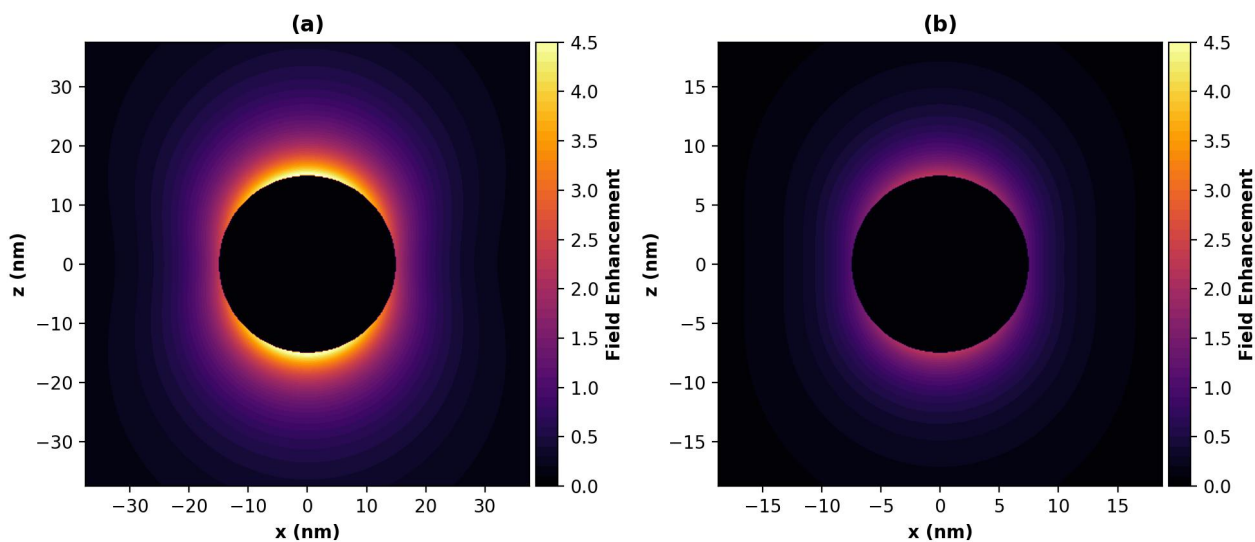


Figure S9: Near-field enhancement factor (scattered electric field amplitude over incident field amplitude) at $\lambda = 410 \text{ nm}$ for (a) 30 nm AgNP and (b) 15 nm AuNP.

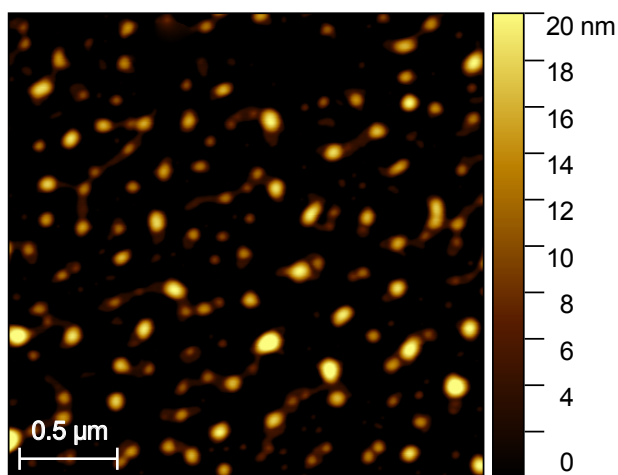


Figure S10: AFM image of P3000-CDs.

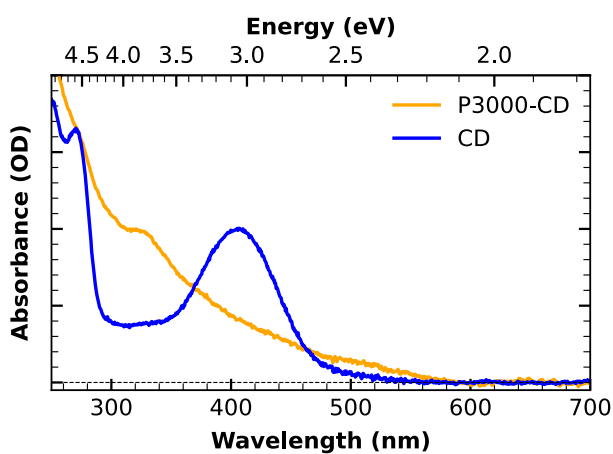


Figure S11: Comparison between absorption spectrum of P3000-CDs (blue) and pristine CDs (orange).

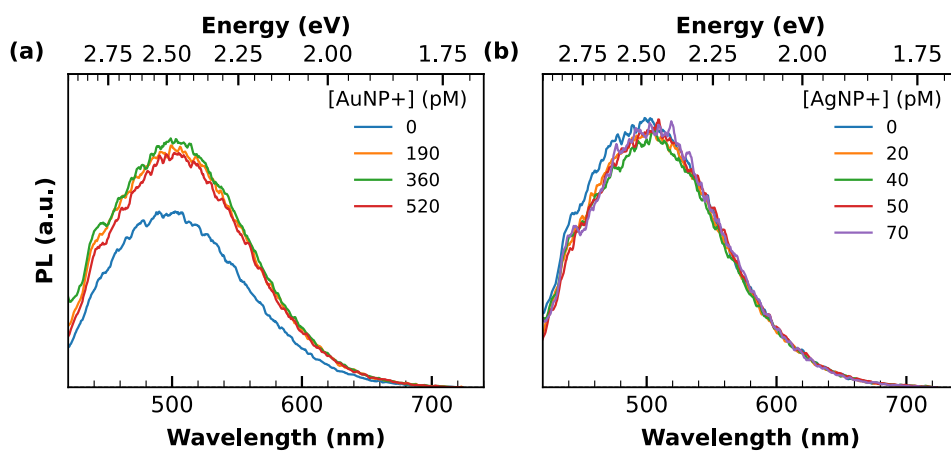


Figure S12: PL spectra of P3000-CD aqueous solution under $\lambda_{exc} = 410 \text{ nm}$ upon increasing concentrations of (a) AuNP+, (b) AgNP+.

References

- [1] Craig F. Bohren and Donald R. Huffman. Absorption and Scattering of Light by Small Particles. 1998.
- [2] Sciortino, A.; Mauro, N.; Buscarino, G.; Sciortino, L.; Popescu, R.; Schneider, R.; Giammona, G.; Gerthsen, D.; Cannas, M.; Messina, F. β -C₃N₄ Nanocrystals: Carbon Dots with Extraordinary Morphological, Structural, and Optical Homogeneity. *Chemistry of Materials* **2018**, *30*, 1695–1700.